Estimating the Fraction of PAR Absorbed by Live Phytoplankton from Satellite Data

Robert Frouin[1], Jing Tan[1], Toru Hirawake[2], B. Greg Mitchell[1], Natalia Rudorff[3], Milton Kampel[3]

[1]Scripps Institution of Oceanography, University of California San Diego, La Jolla, California, USA

[2]Faculty of Fisheries Sciences, Hokkaido University, Hakodate, Japan

[3]Remote Sensing Division, National Institute for Space Research, São José dos Campos, Brazil

---

NASA OCRT Meeting, Busan, Republic of Korea, 08 April 2019

Introduction

-Primary production, *PP*, depends on the fraction of photo-synthetically available radiation, *PAR*, absorbed by live phytoplankton, *APAR*, i.e., $PP = e\ APAR\ PAR$, where e is an efficiency factor for photosynthesis.

-APAR can be expressed as (Kirk 1994):

$$APAR = \int\int\{K_d(\lambda,z)E_d(\lambda,z)\ a_{ph}(\lambda,z)/a_{tot}(\lambda,z)\}d\lambda \ / \int E_d(\lambda,0^-)\ d\lambda$$

where K_d is the diffuse attenuation coefficients, E_d is the spectral solar irradiance below the surface, a_{ph} is the phytoplankton absorption coefficient, a_{tot} is the total absorption coefficient, and the integral is over the PAR spectral range, i.e., 400 to 700 nm, and over the depth z (from surface to the depth of the euphotic zone).

-In the case of a vertically homogeneous water body, *APAR* reduces to:

$$APAR = \int(E_d(\lambda)\ a_{ph}(\lambda)/a_{tot}(\lambda))d\lambda \ / \int E_d(\lambda)d\lambda$$

-Computing *APAR* requires knowledge of $E_d(\lambda)$, $K_d(\lambda)$, $a_{ph}(\lambda)$, and $a_{tot}(\lambda)$.

-$E_d(\lambda)$ can be obtained by adapting existing methods for *PAR* above the surface. This is straightforward since the effect of clouds on transmittance is white in the PAR spectral range (see Frouin et al., 2018).

-$K_d(\lambda)$, $a_p(\lambda)$, and $a_{tot}(\lambda)$ can be obtained from water reflectance, $R_w(\lambda)$, using various techniques; see, e.g., IOCCG, 2005 for absorption coefficients.

-Estimating the various quantities from R_w is accomplished with uncertainties (it is especially difficult to estimate a_{ph}); no vertical information. Algorithms are also sensitive to atmospheric correction errors.

Algorithm Development

-Consider homogeneous case for simplicity. APAR can be re-arranged in terms of R_w as:

$$APAR \approx \int\{E_d(0^-)\,[a_{ph}/(a_{ph} + a_{dm} + a_g)]\,[1 - (R_w(0^-)/R_{w0}(0^-))(f_0/f)(b_{b0}/(b_{b0} + b_{bp})]\}d\lambda \;/\; \int E_d(0^-)\,d\lambda$$

by incorporating the following equations:

$$a_{tot} = a_{ph} + a_{dm} + a_g + a_0,\; R_{w0}(0^-) \approx f_0 b_{b0}/a_0,\; R_w(0^-) \approx f b_b/a_{tot}$$

where a_{dm}, a_g and a_0 are the absorption coefficients for detritus/sediments, colored dissolved organic matter, and pure water, respectively, b_{b0} and b_{bp} are the backscattering coefficients for water molecules and particles, respectively, and R_{w0} is the reflectance for pure sea water.

-This suggests that *APAR* can be approximated by a linear combination of $R_w(0^-)/R_{w0}(0^-)$in the PAR spectral range. Introducing R_{w0} reduces the sensitivity to IOP variability.

APAR versus R_w/R_{w0} from field data

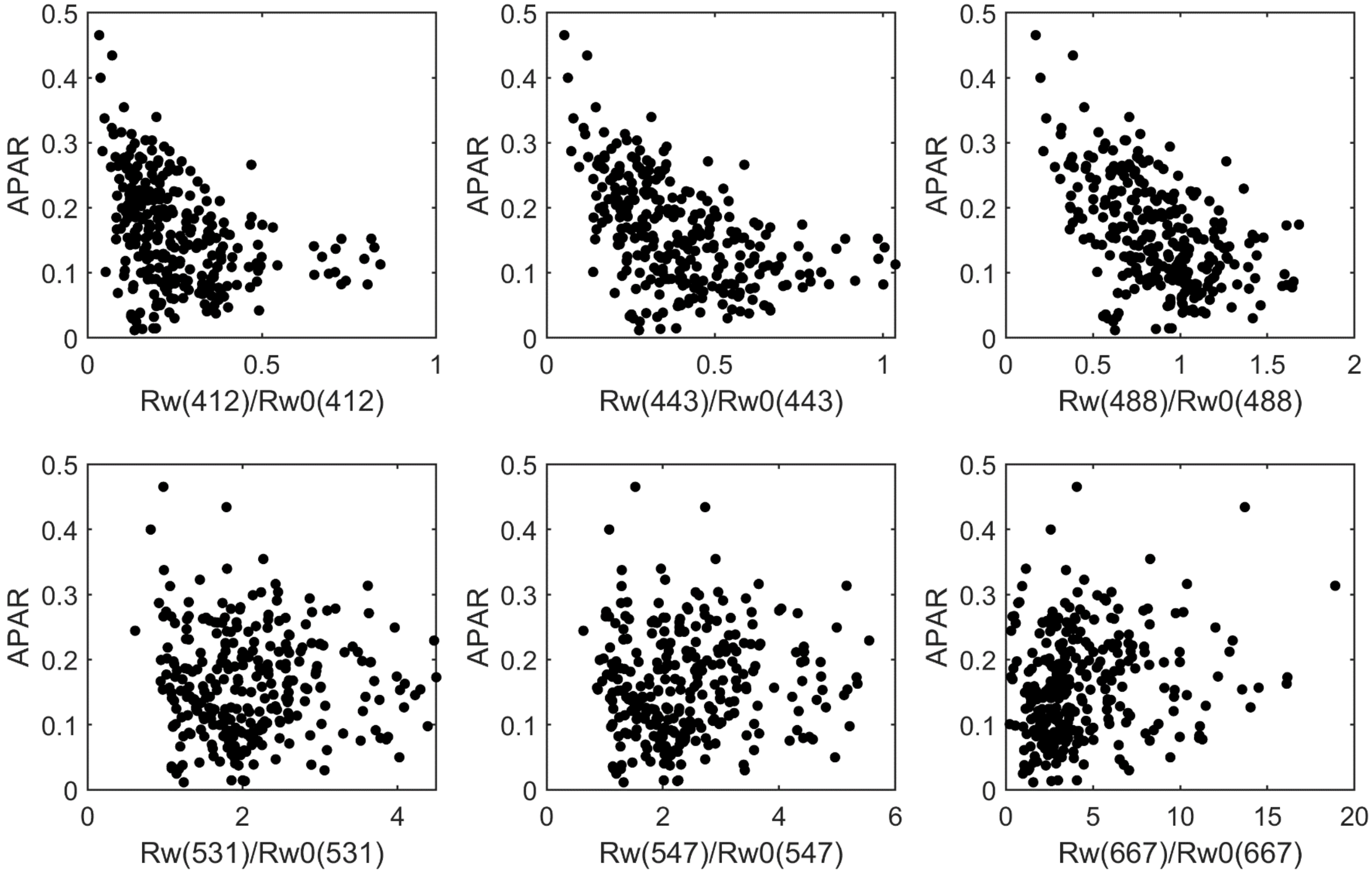

Figure 1*: Relation between APAR versus(R_w/R_{w0} at MODIS wavelengths from field data (SPG archive, other cruises, 294 points).*

Performance of linear R_w/R_{w0} combinations

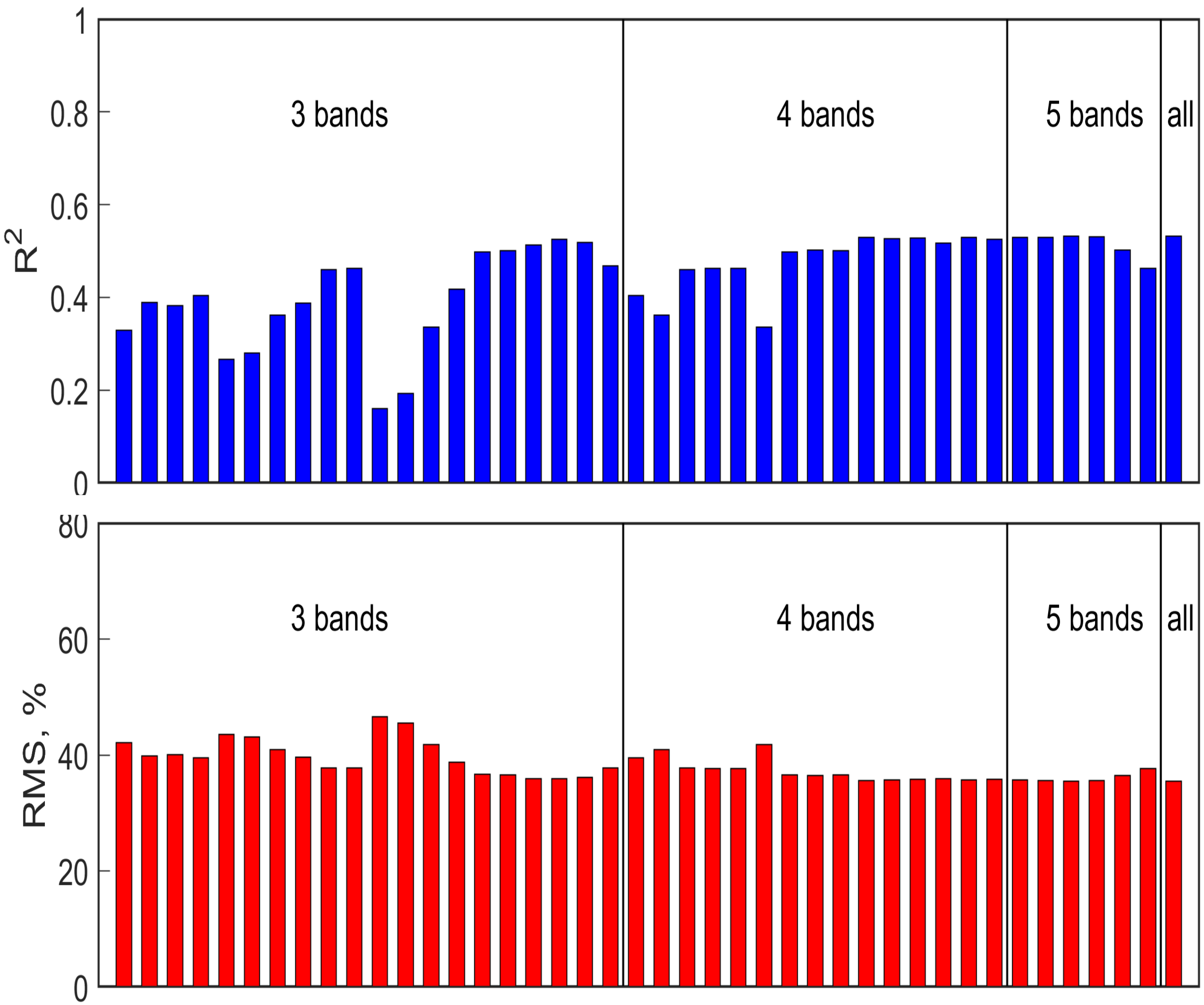

***Figure 2**: R^2 and RMS (%) of estimated APAR using 3-band, 4-band, 5-band, and 6-band combinations when applying systematical examination to in-situ data. APAR is estimated as linear combinations of R_w/R_{w0}. MODIS bands at 412, 443, 531, 547, and 667 are considered.*

Comparison of APAR algorithms
([Chl]-based, QAA-based, and linear R_w /R_{w0} combination)

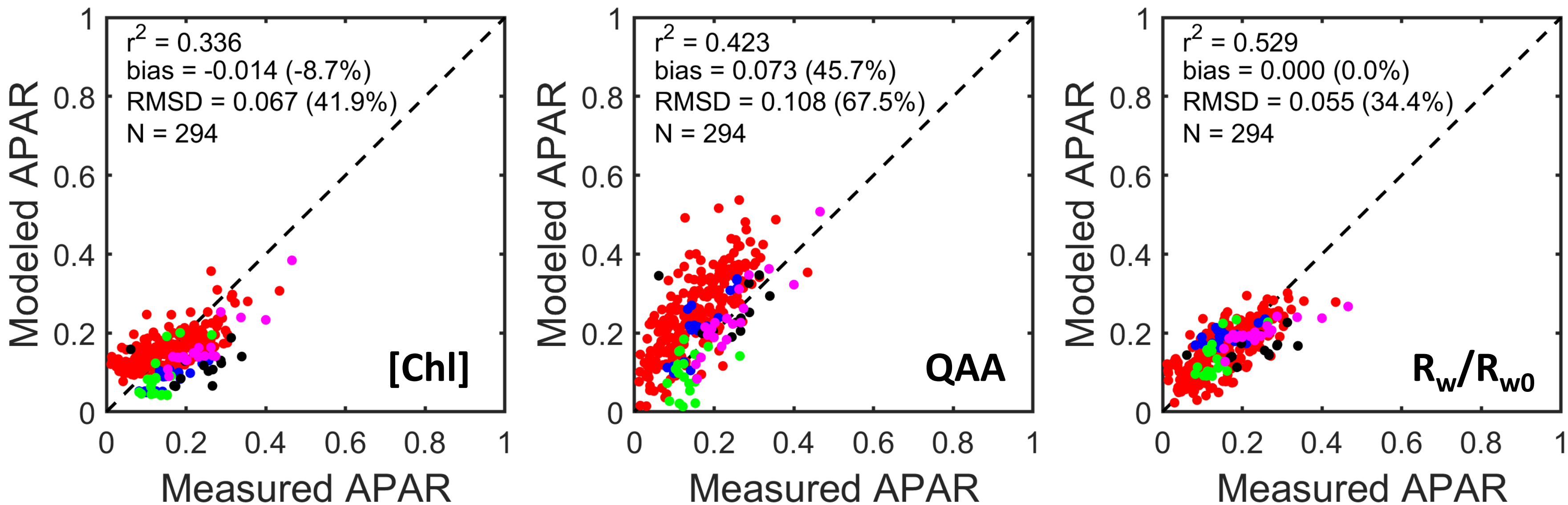

***Figure 3**: Comparison of estimated and "measured" APAR using field data archived in the SPG database(red), collected during BIOSOPE (blue), OUTPACE (green), Japan Sea (black), and MV1102 (magenta) cruises: left - using OC3M-derived [chl] and APAR = a[Chl]^b, middle - using QAA-derived a_{ph} and a_{tot}, and right - using R_w /R_{w0} ratios at 412, 443, 488, 531, 547, and 667 nm.*

-Accuracy is substantially improved using R_w /R_{w0} combination, e.g., RMSD reduced from 67 to 34% compared with QAA-based method.

Robustness of R_w/R_{w0} algorithm to atmospheric correction errors

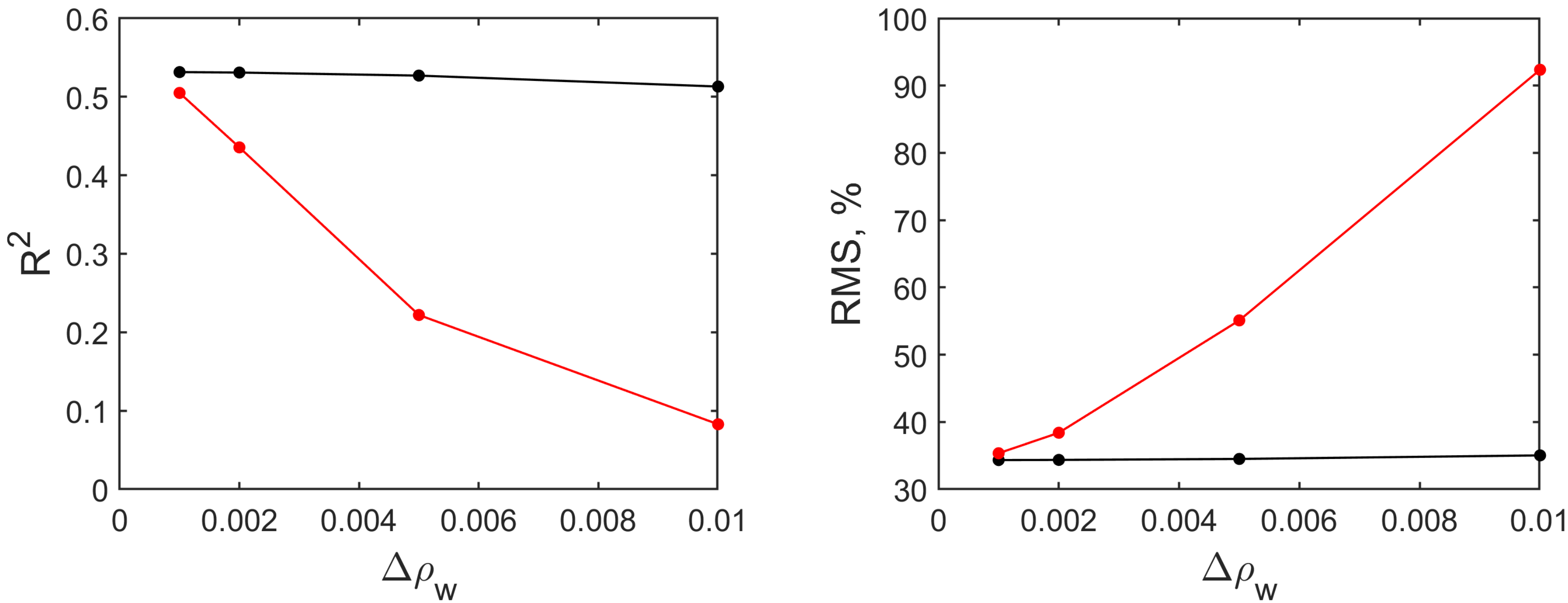

Figure 4: *Sensitivity of the best linear combination (i.e., using 6 bands) to atmospheric noise, which is spectrally correlated (black) and uncorrelated (red). The noise level at 443 nm,* $\Delta\rho_w$ *(*ρ_w *is the water reflectance above surface), varies from 0.001 to 0.01.* R^2 *and RMS (%) are displayed against the APAR calculated using in-situ measurements.*

R_w/R_{w0} algorithm and uncertainty for satellite application

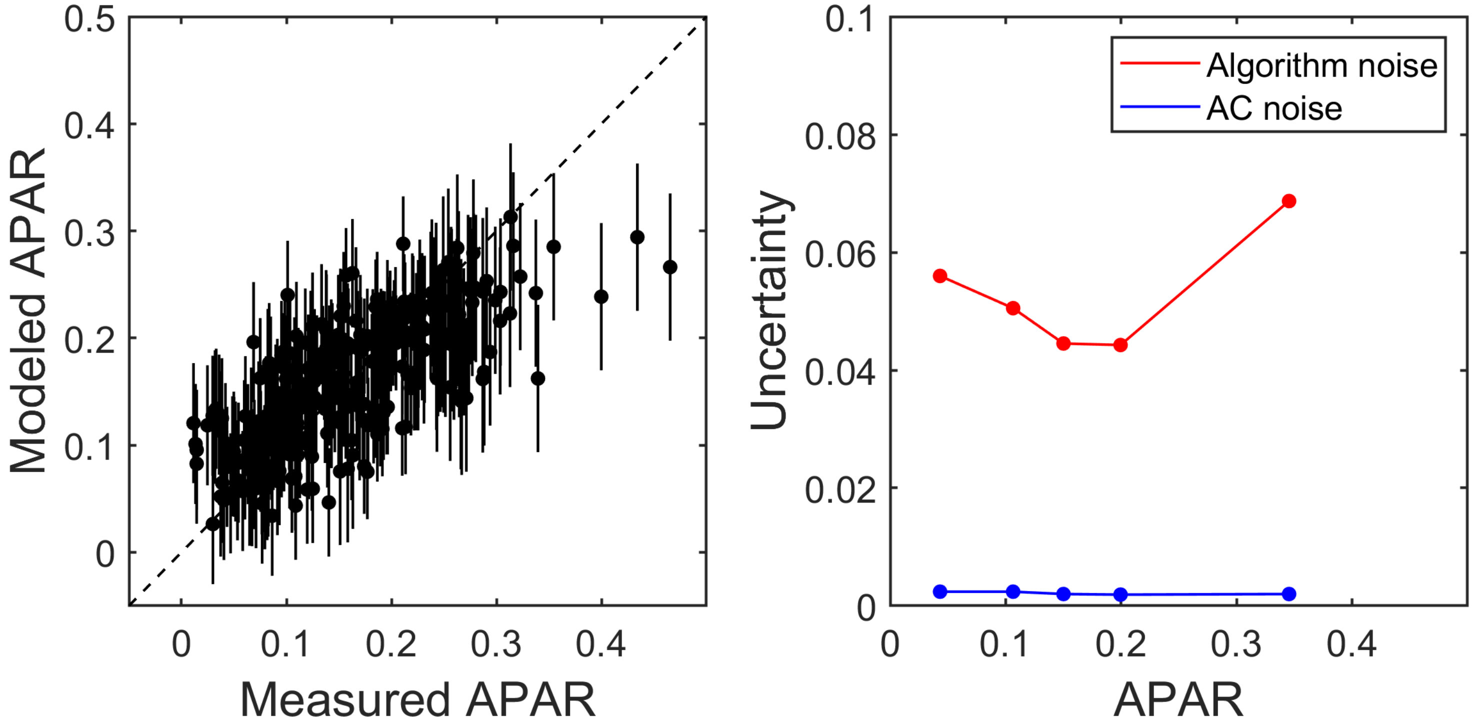

***Figure 5**: Left: comparison of estimated and "measured" APAR using field measurements. Error bars indicate the noise due to spectrally correlated atmospheric noise and algorithm error. Right: APAR uncertainty due to spectrally correlated atmospheric correction noise (blue) and algorithm error (red).*
$APAR=0.1084+1.8385R_w(412)/R_{w0}(412)-2.1448R_w(443)/R_{w0}(443)+0.5785*R_w(488)/R_{w0}(488)-0.1935R_w(531)/R_{w0}(531)+0.1141R_w(547)/R_{w0}(547)-0.0008R_w(667)/R_w(667).$

Application to L2 MODIS imagery, Patagonia, March 26, 2019

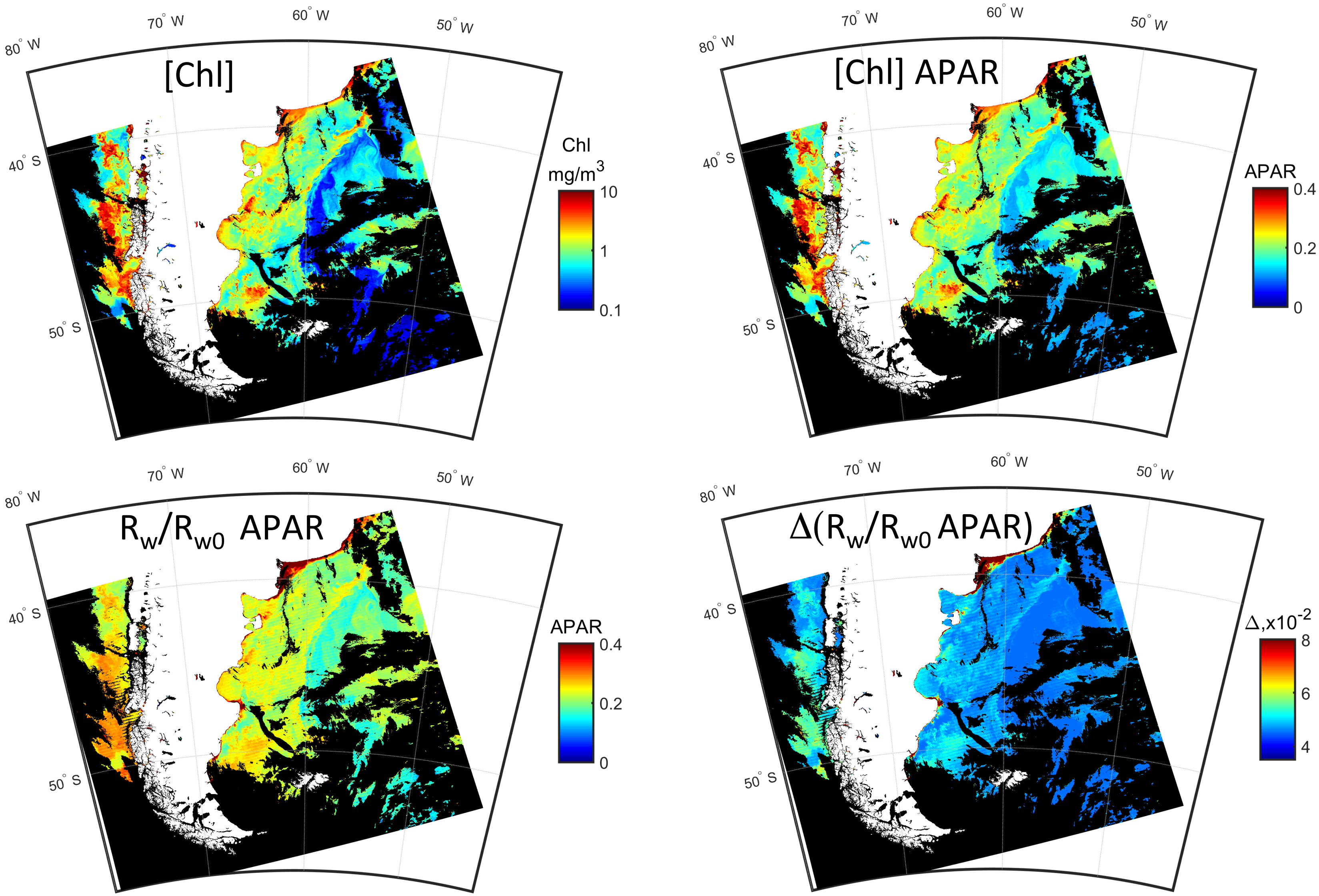

***Figure 6**: Application of APAR algorithms to MODIS-A imagery of March 26, 2019. Top left: [Chl]; Top right: [Chl]-based APAR; Bottom left: R_w/R_{w0}-based APAR; Bottom right: uncertainty on R_w/R_{w0}-based APAR. Land is in white and missing data in black.*

Average APAR from MODIS global L3 imagery, March 2018

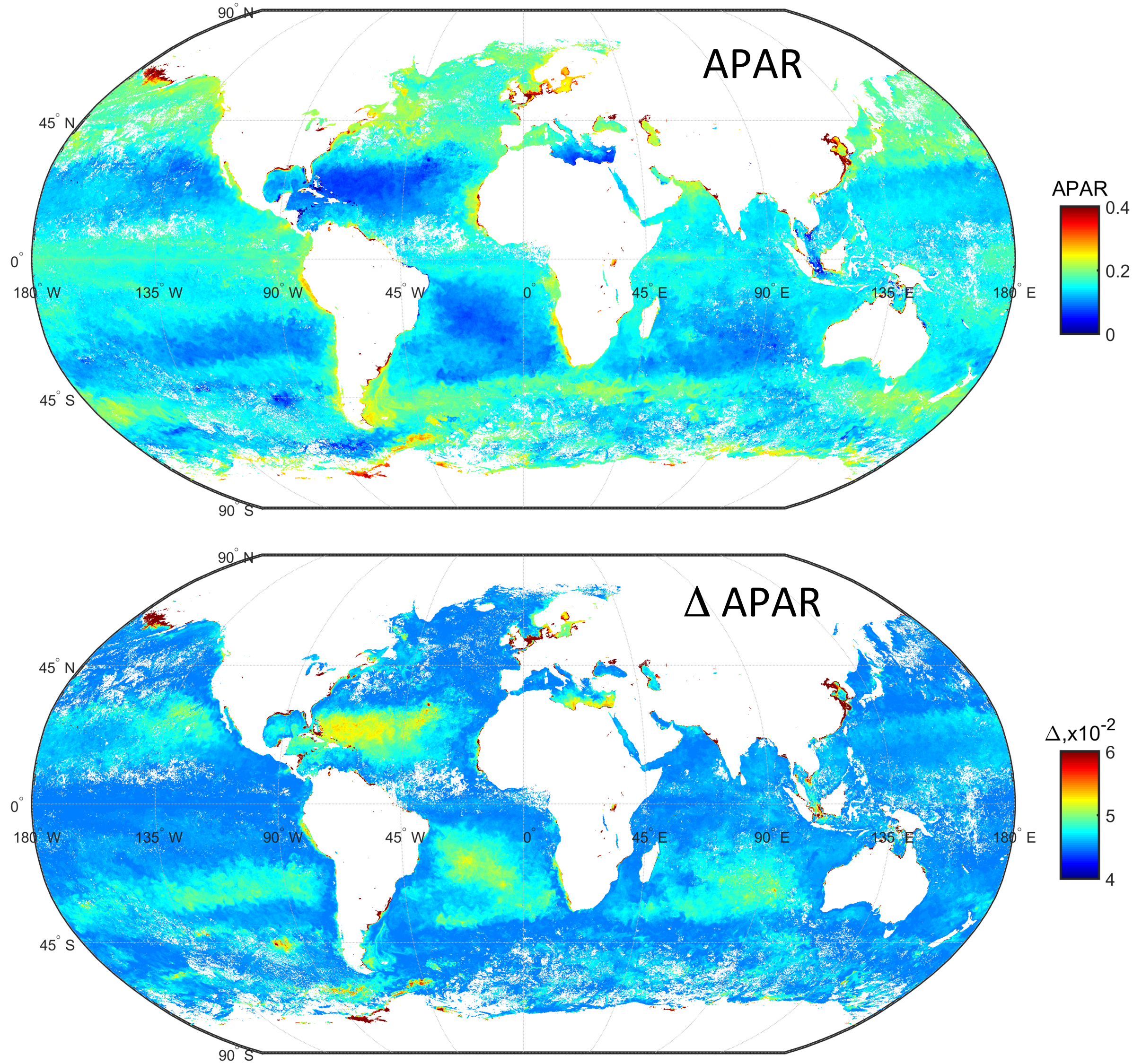

Figure 7: *Monthly average APAR (March 2018) estimated from MODIS L3 imagery by the R_w/R_{w0} algorithm and associated uncertainty (top and bottom, respectively.*

-To improve APAR estimates, one may classify reflectance spectra, and for each class use a separate linear R_w/R_{w0} combination.

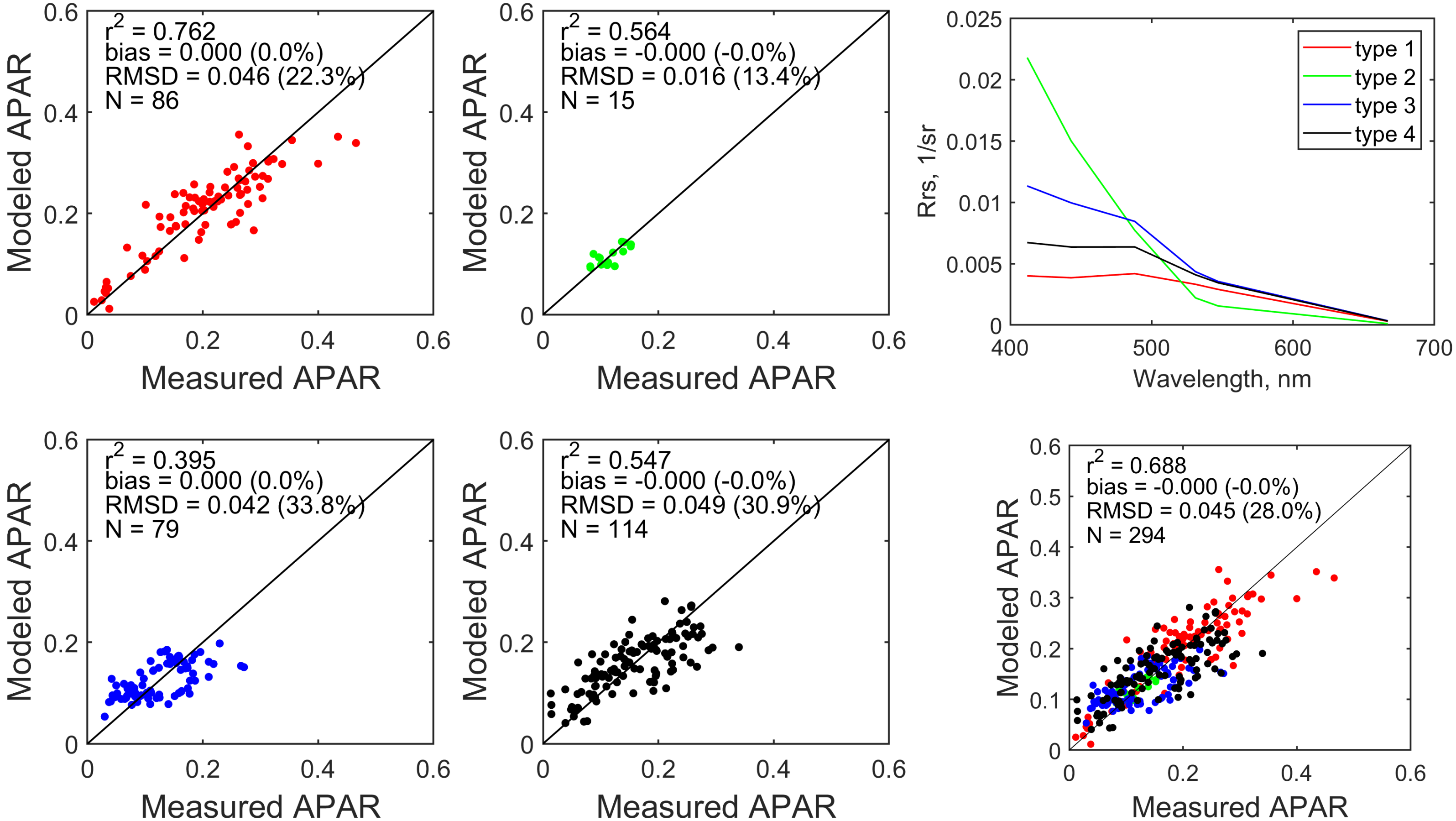

***Figure 8**: Top right: Average reflectance spectra for 4 classes obtained using k-means. Left: Modeled versus measured APAR for each class. The coefficients of estimating APAR are determined based on specific water class, using all 6 bands. Right: Modeled versus measured APAR, all four water classes together. RMSD is reduced from 34 to 28% and R^2 is increased from 0.53 to 0.69 when using classification.*

Class-based linear R_w/R_{w0} combination, Patagonia, March 26, 2019

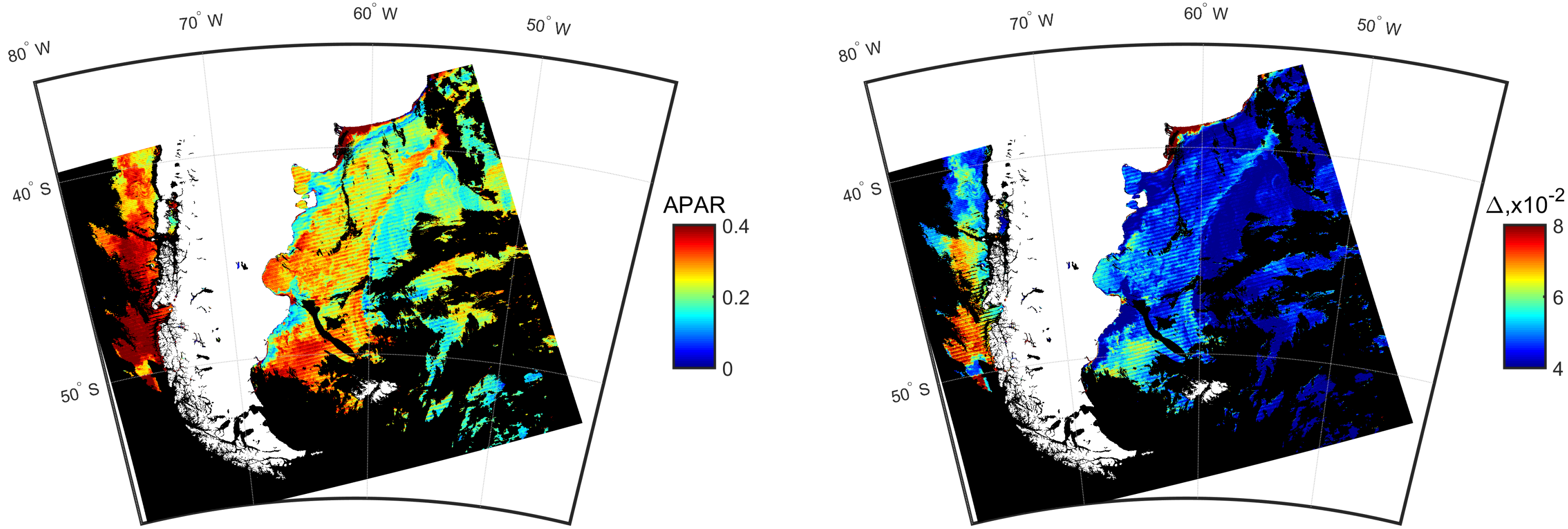

Relative frequency, *[Chl]* and linear R_w/R_{w0} combination algorithms

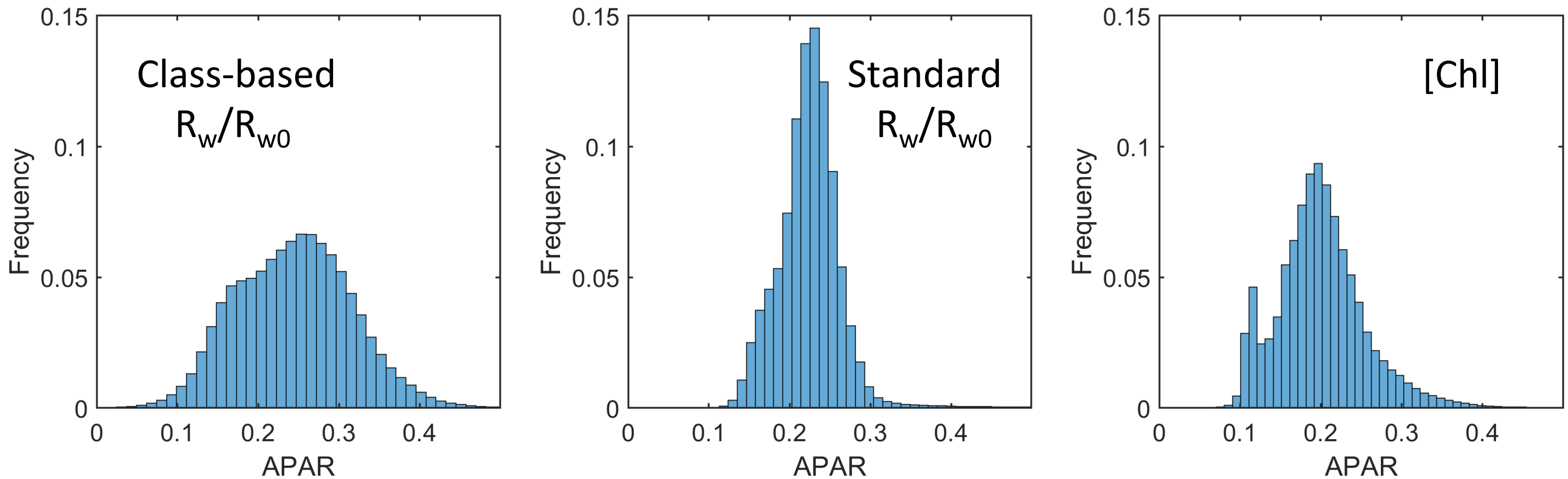

Figure 9: *Top: Spatial maps of APAR and associated uncertainties obtained by the class-based R_w/R_{w0} algorithm (MODIS March 26, 2019, Patagonia) . Bottom Relative frequency histograms for [Chl] and R_w/R_{w0} algorithms (class-based and standard).*

Classification using simulated data set (IOCCG, 2005)

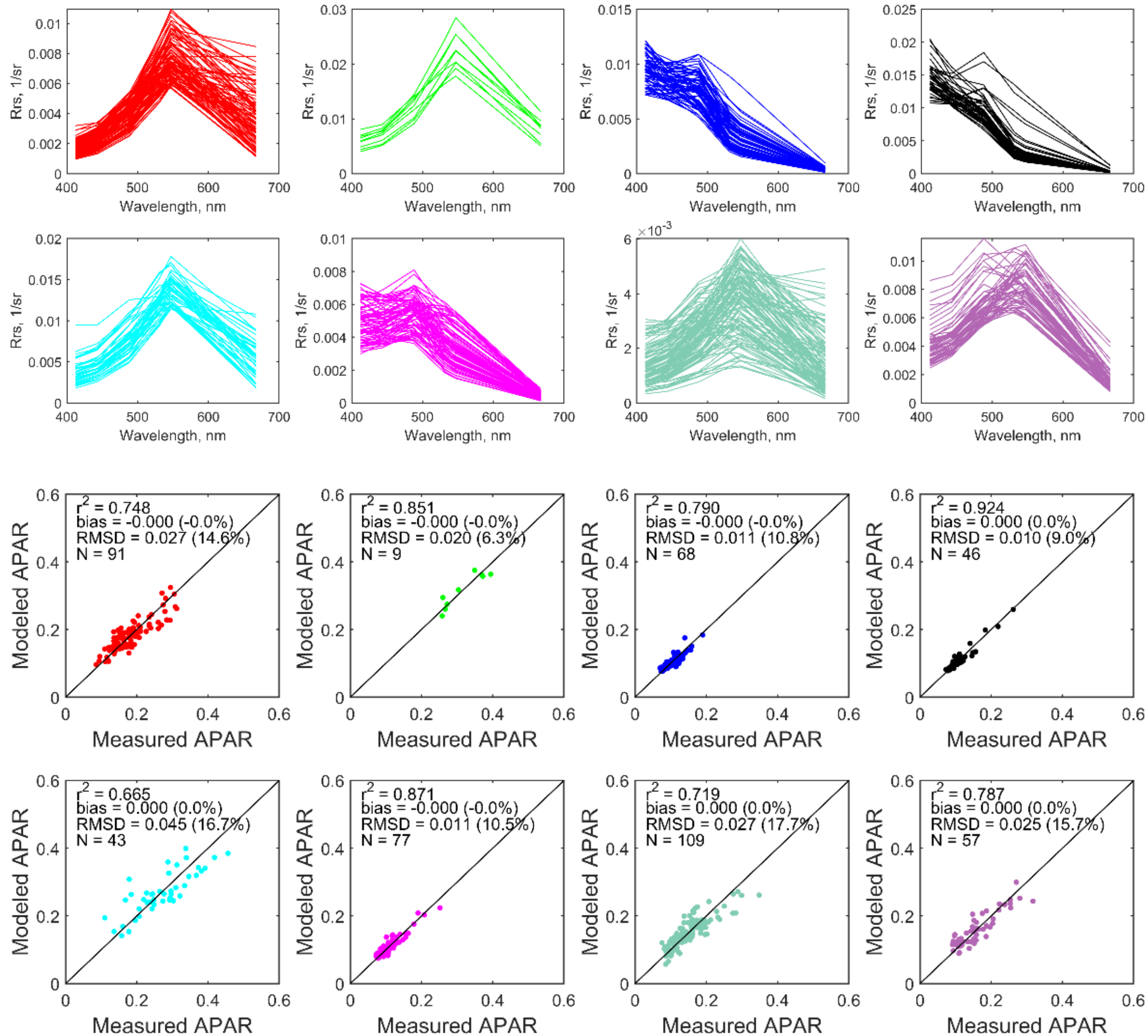

***Figure 10**: Water reflectance classes (top) and performance of linear R_w/R_{w0} combinations for each class (bottom) using IOCCG data set (500 situations).*

Theoretical performance (IOCCG data) and evaluation (in situ data)

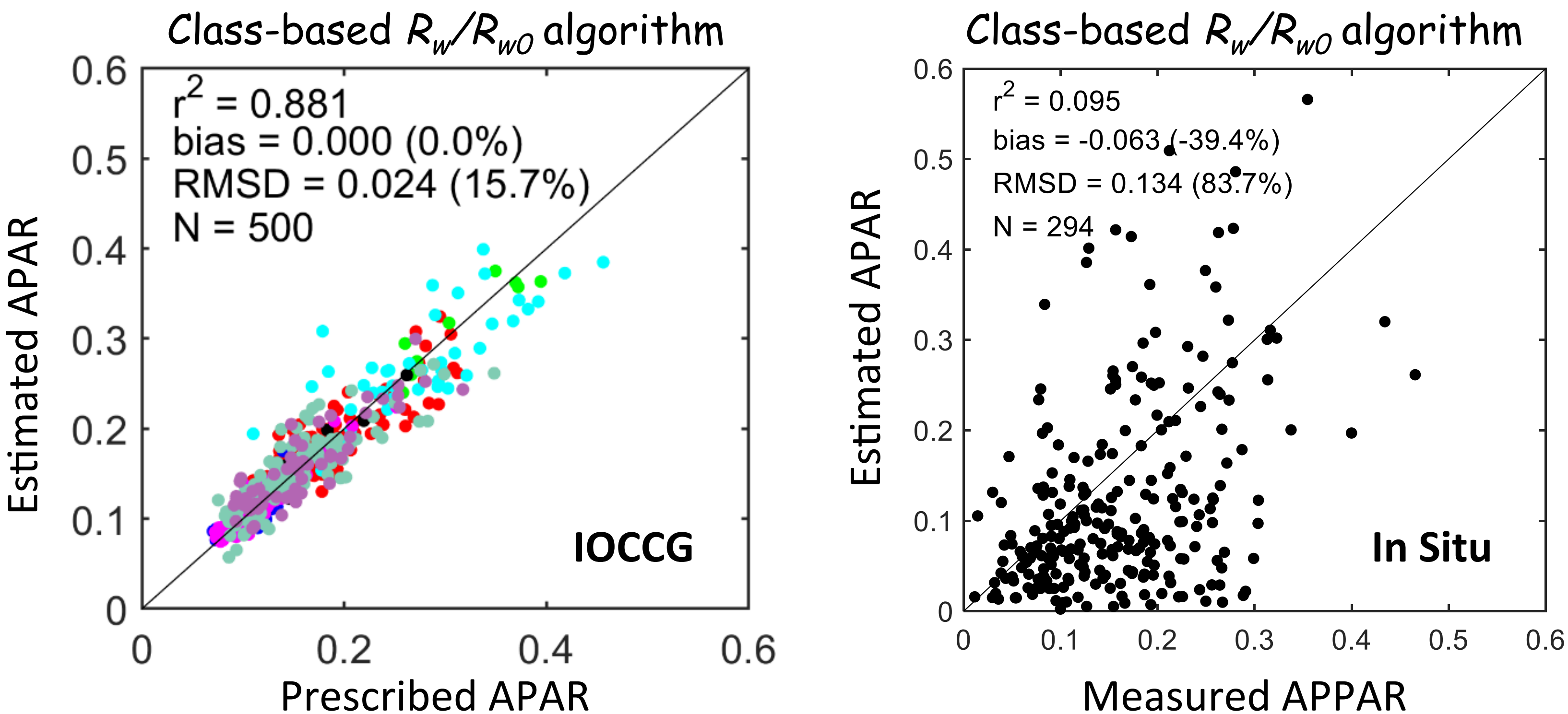

***Figure 11**: Theoretical performance of class-based APAR linear R_w/R_{w0} algorithm on IOCCG data, all classes (left) and evaluation on in situ data (right). IOCCG data set may not represent well in situ situations.*

Summary/Conclusions

-APAR can be derived directly from a linear combination of R_w/R_{w0} in the PAR spectral range. Spectral absorption coefficients, K_d, and E_d do not need to be determined.

-For MODIS, 6 spectral bands (412, 443, 488, 531, 547, and 667) yields the most accurate estimates.

-Accuracy is improved compared with *[Chl]*- and QAA-based algorithms, e.g., RMS difference reduced to 34% instead of 42 and 67%, respectively.

-Algorithm is very robust to spectrally correlated atmospheric correction errors.

-Classifying reflectance and using a linear R_w/R_{w0} combination for each class is promising to reduce the impact of IOP variability and improve APAR estimates.

-A more comprehensive in situ dataset is needed to generalize the results. Simulated data may fill data gaps, and allow more robust *APAR* determinations per class, the subject of future work.